Atmospheric Research 210 (2018) 41–57

Contents lists available at ScienceDirect

Atmospheric Research

journal homepage: www.elsevier.com/locate/atmosres

Lightning climatology over the northwest Pacific region: An 11-year study using data from the World Wide Lightning Location Network

Wenjuan Zhang[a,*], Yijun Zhang[b], Dong Zheng[a], Liangtao Xu[a], Weitao Lyu[a]

[a] State Key Laboratory of Severe Weather, Chinese Academy of Meteorological Sciences, Beijing, China
[b] Institute of Atmospheric Sciences, Fudan University, Shanghai, China

ARTICLE INFO

Keywords:
Lightning climatology
Northwest Pacific
WWLLN
Tropical cyclone
ENSO

ABSTRACT

Lightning data from the World Wide Lightning Location Network for the period 2005–2015 were used to investigate climatic characteristics of lightning activity over the northwest Pacific region (0°–55°N, 100°–180°E). The highest lightning densities (LDs) were observed over the coastal areas of southeast Asia and the tropical islands, which differs significantly from the distribution of the highest precipitation rates. The LD in the South China Sea (SCS) was much higher than that over the deep ocean and showed a peak that was 3 h ahead of that seen in the open sea. A sharp increase in LD on the Indo-China Peninsula and in the SCS was observed during the pre-monsoon season. The monthly variations show that the highest lightning activity occurred during July, August, and September, which is consistent with the variations in the monthly precipitation rate.

The contribution of tropical cyclones (TCs) and the impact of El Nino and La Nina events on lightning climatology over the northwest Pacific region were also examined. Two areas of maximum TC lightning were observed to the east of the Philippines and south of China, indicating that frequent lightning is produced when TCs are approaching landfall. The average LD during El Nino events increases by 10.3%, whereas during La Nina events it decreases by 4.8%. A northward shift in the positive lightning anomaly was observed in the SCS, from the southern SCS during the El Nino to the central and northern SCS during the La Nina periods.

1. Introduction

As cloud electrification is closely related to deep convection in thunderstorms, the climatology of lightning activity has been widely studied to reveal the climatic characteristics of thunderstorms and convective systems, both at regional (e.g., Kandalgaonkar et al., 2005; Kuleshov et al., 2006; Poelman, 2014) and global scales (e.g., Christian et al., 2003; Cecil et al., 2015; Albrecht et al., 2016), as well as over land (e.g., Orville and Huffines, 2001; Qie et al., 2003; Yang et al., 2015) and ocean (e.g., Hidayat and Ishii, 1998; Altaratz et al., 2003; Bovalo et al., 2012). This study focuses on lightning climatology over the northwest Pacific region, but the study domain extends beyond the ocean to cover the area of 0°–55°N and 100°–180°E. Therefore, the distribution of lightning over the entire life cycle of tropical cyclones (TCs) generated over the northwest Pacific Ocean, as well as the contrast in lightning activity between the ocean and the land, can be investigated. This region covers East/Southeast Asia, the South China Sea (SCS), the deep ocean of the northwest Pacific, and tropical islands of the Maritime Continent (MC).

The northwest Pacific region is affected by a variety of climatic systems and shows unique weather patterns. Due to the Asian monsoon, this region is a significant monsoon-affected area in the world. Convection over this region during the monsoon season is a significant contributor of precipitation and heat in the Northern Hemisphere (Johnson and Ciesielski, 2002). The northwest Pacific region is also the most active TC basin globally, and experiences the largest number of intense tropical storms. Moreover, the northwest Pacific region is an El Nino Southern Oscillation (ENSO)-sensitive area, which is indicated by the great contrast in convection between the El Nino and La Nina events (Curtis and Adler, 2003). Investigation of lightning climatology over the northwest Pacific region could help to improve our understanding of the occurrence and variability of intense convections and thunderstorms in this region.

Decade years of observations by the Tropical Rainfall Measuring Mission (TRMM) satellite have allowed climatological studies of global lightning activity. Global lightning maps (e.g., Christian et al., 2003; Cecil et al., 2015) based on data from the Lightning Imaging Sensor (LIS) and Optical Transient Detector (OTD) describe that the northwest Pacific region is an area of high lightning occurrence, with Malaysia and Indonesia being the global lightning hotspots (Albrecht et al.,

* Corresponding author.
E-mail address: zwj@cma.gov.cn (W. Zhang).

https://doi.org/10.1016/j.atmosres.2018.04.013
Received 30 October 2017; Received in revised form 3 April 2018; Accepted 13 April 2018
Available online 01 May 2018
0169-8095/ © 2018 Elsevier B.V. All rights reserved.

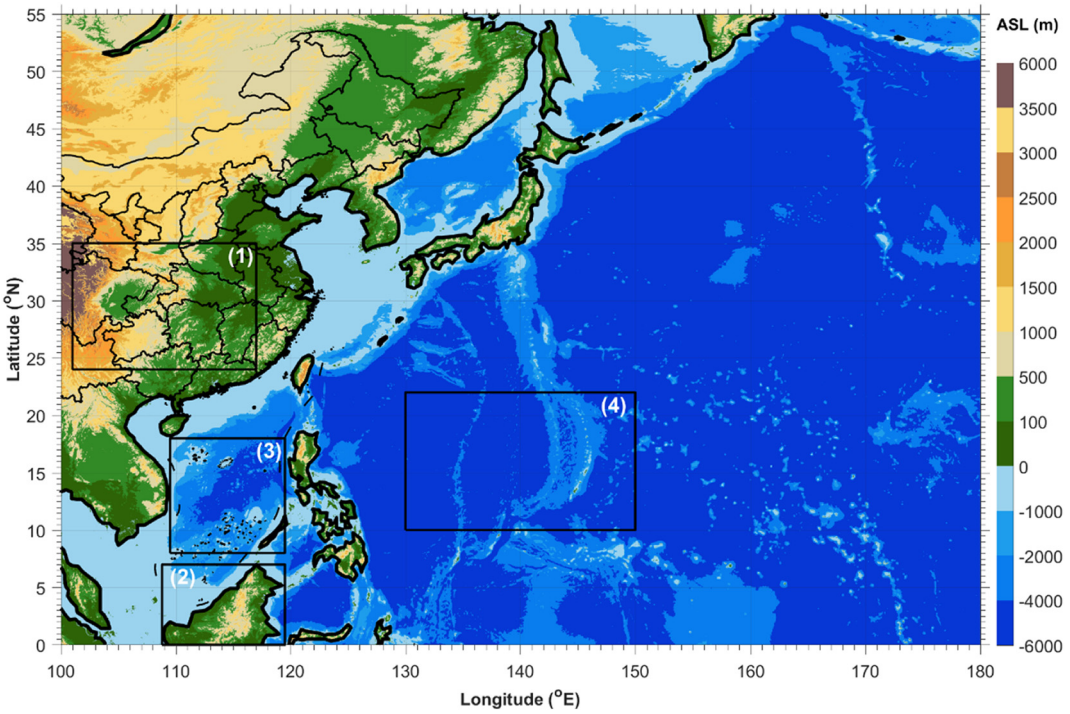

Fig. 1. Plan view of the northwest Pacific region analyzed in this study overlaid terrain elevation (m). Designated (1) inland, (2) tropical islands, (3) the South China Sea, and (4) the open sea with boxes are sampled for diurnal variation.

2016). Other studies have used ground-based lightning detection networks to investigate regional lightning activity across the northwest Pacific region. These studies reported high flash rates on tropical islands including Malaysia (Venugopal et al., 2016) and Indonesia (Hidayat and Ishii, 1998), an unusually high frequency of lightning strokes during winter season in Japan (Iwasaki, 2014; Tsurushima et al., 2017), and a high flash density during the monsoon season in Southeast China (Yang et al., 2015; Zheng et al., 2016). Since the northwest Pacific region is an area with large lightning occurrence, more detailed analysis of climatological lightning activity, in terms of the spatial, seasonal, and diurnal distributions, is required.

Frequent lightning has been observed in TCs (or typhoons) in the northwest Pacific Ocean over the last two decades. Lightning was originally considered to be sparse in tropical storms, because there is little supercooled water above the melting level and a lack of ice particles in tropical clouds (Willoughby et al., 1982; Black and Hallett, 1986). With the development of lightning detection systems in Asia, as well as the global network, more and more studies have highlighted that lightning in TCs in the northwest Pacific is a common event. Pan et al. (2010) first described intense lightning activity in super typhoons over the northwest Pacific. Hereafter high lightning densities (LDs) were also observed in weaker intensity storms as tropical depressions and tropical storms (Zhang et al., 2015). Lightning flash rate was found to be related to TC intensity (Pan et al., 2014). Lightning outbreaks in the eyewall/inner core were found to be an indicator of TC intensification (Zhang et al., 2012). Case studies (Zhang et al., 2013; Wang et al., 2016) of Typhoon Molave (2009) and Super Typhoon Haiyan (2013) also highlighted the relationship between lightning and TC intensity changes, and described in detail the lightning characteristics associated with the evolution of TC convection. These previous studies focused mainly on the lightning distribution in typhoons and its relationship with TC intensity. The contribution of TCs to the climatological lightning over this region has not been studied yet.

El Nino and La Nina events are anomalous climate phenomena within the global ocean-atmosphere system. This is supported by the evidence that sea surface temperatures (SST) over the central and eastern Pacific Ocean are higher or colder than normal. Accompanied by the eastward migration of the warm pool, El Nino causes a shift in convective activity from the western to the central and eastern Pacific (Curtis and Adler, 2003). La Nina event generally appears after El Nino, with a cooling of the SST in the same areas. The major impacts of El Nino/La Nina over the northwest Pacific region are variations in the magnitude of convective storms (Curtis and Adler, 2003; Kumar and Kamra, 2012), suppressed convective rainfalls (Hamid et al., 2001), changes in precipitation patterns (Yoshida et al., 2007), and enhancement of storm intensity (Hamid et al., 2001; Williams, 2005). Since lightning is closely linked to storm intensity and deep convection, connections between lightning activity and El Nino/La Nina events have been found over this region. The number of lightning flashes was found to be increased during the El Nino periods in southern China (Ma et al., 2005), South/Southeast Asia (Kumar and Kamra, 2012), and the Western Pacific and the MC (Hamid et al., 2001). In contrast, during the La Nina periods, lightning activity was reported to be decreased over the same areas (Yoshida et al., 2007; Kumar and Kamra, 2012). Lightning and convection have shown a southeastward shift during the El Nino events in South/Southeast Asia (Kumar and Kamra, 2012). In addition, the spatial distribution of positive anomalies is found to be varied with the seasons (Ma et al., 2005).

The objective of this paper is to study the climatology of lightning activity over the northwest Pacific region (0°–55°N, 100°–180°E). Using 11-year of World Wide Lightning Location Network (WWLLN) data covering the period 2005–2015, we will seek to understand: (a) the spatial distribution and the seasonal and diurnal variations of lightning activity over this region, (b) the contribution of TCs to the climatological lightning, and (c) the impact of El Nino and La Nina events on lightning activity over this region. The remainder of the paper is organized as follows. Section 2 introduces the data and methodology used in this study. Section 3 provides the results and discussion. The conclusions are given in Section 4.

2. Data and methodology

2.1. Study domain

The analysis domain for this study was geographically restricted to the region enclosed by 0°–55°N and 100°–180°E and covers the northwestern Pacific Ocean and East/Southeast Asia. For the investigation of diurnal variations, four sub-regions (Fig. 1) were chosen to study the lightning characteristics over the inland area (24°–35°N, 101°–117°E), the tropical islands (0°–7°N, 109°–120°E), the SCS (8°–18°N, 110°–120°E), and the open sea (10°–22°N, 130°–150°E).

2.2. Lightning data

The lightning data used in this study covered the period 2005–2015 were extracted from the WWLLN database. The WWLLN monitors lightning strokes around the globe in real time using VLF receivers. The network determines lightning locations with at least five sensors and gives lightning information on time, latitude, and longitude (Rodger et al., 2004). As of January 2013, the WWLLN has consisted of over 70 stations around the world (Hutchins et al., 2013). The increasing number of stations has led to an improvement in detection efficiency (DE) to approximately 11% (Rudlosky and Shea, 2013; Virts et al., 2013b). Further details of the WWLLN can be found in Dowden et al. (2002), Lay et al. (2004), Rodger et al. (2005), Jacobson et al. (2006), Abarca et al. (2010), and Hutchins et al. (2012).

The WWLLN and LIS are the only two datasets that offer observations of global lightning for > 10 years. LIS observations identify only snapshots of lightning and are limited to a certain latitude range (± 38°). Despite the lower DE, the sample sizes of the WWLLN are two orders of magnitude larger than those of the LIS (Virts et al., 2013b). Previous studies have confirmed the consistency between the WWLLN and LIS datasets (e.g., Pan et al., 2013; Virts et al., 2013b), and used WWLLN data to investigate lightning climatology for different regions (Lay et al., 2007; Kucienska et al., 2010; Virts et al., 2011, 2013a, 2013b; Bovalo et al., 2012; Garreaud et al., 2014; Venugopal et al., 2016; Soula et al., 2016; Iwasaki, 2016).

As WWLLN DE varied considerably over the period 2005–2015, a method of data conversion from WWLLN stroke to TRMM LIS/OTD flash was required. DeMaria et al. (2012), Stevenson et al. (2018), Bovalo et al. (2012), Bovalo et al. (2014), Pan et al. (2014) and Zhang et al. (2015) used the High Resolution Full Climatology (HRFC) data from the TRMM LIS/OTD to adjust their results from WWLLN in the Atlantic, East Pacific, South-West Indian, and northwest Pacific Oceans. In this study, we used the same WWLLN calibration procedures. It is assumed that variations in LD averaged over large spatial areas are much smaller than the changes due to increase of WWLLN stations and improvements of station coverage. Another assumption is that the ratio of WWLLN stroke to flash is uniform over the analysis period and region. First, the annual average LD of WWLLN was calculated for each year over the domain. Then, the ratios between these values and the annual lightning climatology over the same domain from LIS/OTD were calculated as adjustment factors (or conversion factors). Finally, for each year of the study, the LDs from the WWLLN data were multiplied by the adjustment factors for that year to make the annual average LD equal to that from the LIS/OTD climatology. Because the LIS/OTD climatology is for total lightning, all of the LDs used in this study including adjustment factors were considered to be converted to total LDs. Thus, LD in this study was reported in the units of flashes per square kilometer per year (fl $km^{-2} yr^{-1}$). Table 1 lists the adjustment factors for WWLLN lightning in the domain. The yearly variations in the adjustment factors were believed to be due to increases in the number of WWLLN stations over the northwest Pacific region.

2.3. Tropical cyclone best-track data

TC best-track data were used to define TC lightning and quantify the contribution of TC lightning to the total amount of lightning occurring in the domain. The best-track data were obtained from the Shanghai Typhoon Institute of the China Meteorological Administration. This dataset (Song et al., 2010) provides, at 6-h interval, the storm's central latitude, longitude, the maximum sustained surface wind speed, and the minimum central pressure. TC center locations at hourly intervals were obtained via spline interpolation to estimate the position of lightning relative to the storm center. In this study, 258 TCs between 2005 and 2015 over the northwest Pacific were examined, including 61 tropical storms (TS, 17.2–24.4 m s^{-1}), 52 severe tropical storms (STS, 24.5–32.6 m s^{-1}), 36 typhoons (TY, 32.7–41.4 m s^{-1}), 45 severe typhoons (STY, 41.5–50.9 m s^{-1}), and 64 super typhoons (SuperTY, ≥ 51.0 m s^{-1}). The best tracks of the 258 TCs are presented in Fig. 2.

2.4. Precipitation data

Precipitation data from 2005 to 2015 were derived from the TRMM 3B42 dataset. The dataset generates gridded precipitation rates at a temporal resolution of 3 h and a spatial resolution of 0.25°.

2.5. Environmental data

The National Center for Environment Prediction–National Center for Atmospheric Research (NCEP–NCAR) reanalysis data from 2005 to 2015 were used to assess the environmental conditions. The monthly mean data at a resolution of 2.5° for wind and specific humidity were used for the climatological analysis.

2.6. Analysis methods

In this study, the lightning results are presented in terms of LD (fl $km^{-2} yr^{-1}$), which is obtained by dividing the number of lightning within a grid by the grid area and the number of years analyzed. The grid resolution was confined to 0.25°, to be consistent with the resolution of the TRMM 3B42 data. Previous studies (e.g., Hidayat and Ishii, 1998; Enno, 2011; Makela et al., 2011; Taszarek et al., 2015; Zheng et al., 2016) of lightning climatology have used resolutions ranging from 0.1° to 0.5° for lightning datasets from ground-based networks. The WWLLN detects strokes with an average accuracy of 5 km over the northwest Pacific region (Hutchins et al., 2013; Virts et al., 2013b). Therefore, we believe that 0.25° is an appropriate grid resolution for our database. This grid resolution was also used by Kucienska et al. (2010), Virts et al. (2013b, 2015), and Venugopal et al. (2016) to study WWLLN lightning climatology over the Gulf of Mexico, globally, and the tropics, respectively.

TC lightning is defined as the strokes within 500 km of the hourly interpolated storm center. A number of studies have described the radial distribution of lightning activity in TCs and the values of TC radius varied among the studies. For Atlantic and East Pacific TCs, the radii of about 300 km (e.g., Molinari et al., 1999; Squires and Businger, 2008; Abarca et al., 2011) or 500 km (e.g., DeMaria et al., 2012; Xu et al., 2017) were considered as boundaries of outer rainbands. For the northwest Pacific TCs, radius of 500–600 km (mostly 500 km) were usually selected for the study of TC lightning (e.g., Pan et al., 2014; Zhang et al., 2012; Zhang et al., 2013; Zhang et al., 2015). Pan et al. (2014) found the radii of typhoons over the northwest Pacific Ocean varied from 600 to 1300 km, while 80% were within 600 km according to the satellite images. Zhang et al. (2012, 2015) found that the majority of lightning occurred within 500 km of TCs over the northwest Pacific. Based on the electrical characteristics in preliminary results for the northwest Pacific TCs, in this work, the radius of 500 km was chosen to be TC boundary. This radial extent is closed to the results by Jiang et al. (2013), who found the mean extent of 502 km for outer

Table 1
The adjustment factors for the WWLLN data for each year over the northwest Pacific region (0°–55°N, 100°–180°E) based on lightning densities from the LIS/OTD climatology. DE means the ratio of detected-WWLLN strokes to detected-LIS flashes.

Year	2005	2006	2007	2008	2009	2010	2011	2012	2013	2014	2015
Adjustment factor	17.6	13.0	14.4	10.4	7.8	6.4	6.7	6.1	5.4	5.4	5.8
DE (%)	5.7	7.7	7.0	9.6	12.8	15.5	14.9	16.4	18.4	18.4	17.3

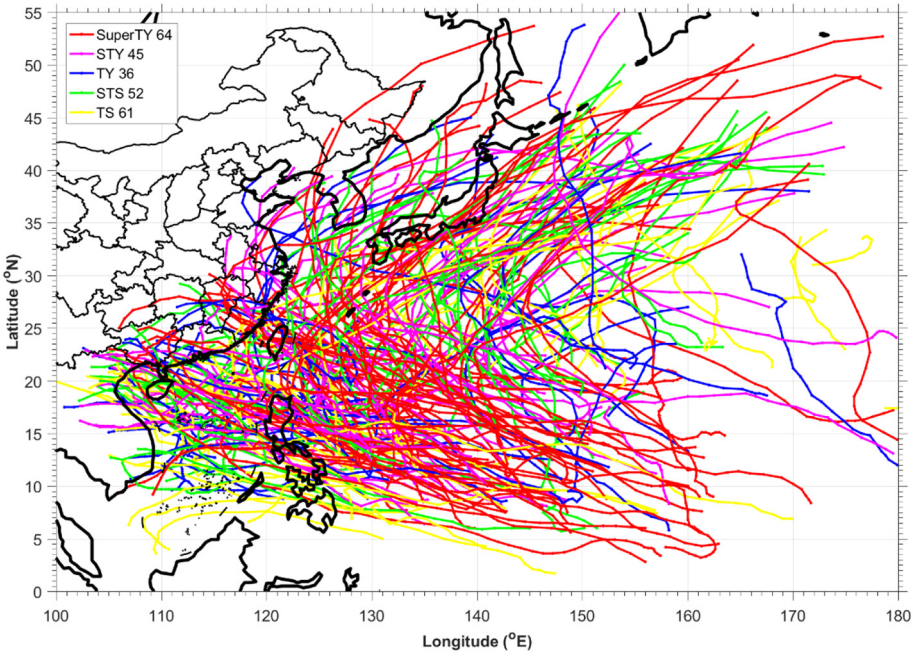

Fig. 2. Best tracks for tropical cyclones between 2005 and 2015 over the northwest Pacific investigated in this study.

rainbands from 11-year observation of TRMM TC overpasses.

For the analysis of diurnal cycle, the number of lightning flashes at local time (LT) were counted in the four designated areas in Fig. 1. LT is defined according to the location of each lightning stroke. The LD (fl km^{-2} day^{-1}) was calculated by dividing the lightning counts by the area and the number of days in the winter season (December, January, and February) or the monsoon season (June, July, August, and September).

To investigate the impact of El Nino and La Nina events, we used the National Standard GB/T 33666-2017 (Ren et al., 2017) to identify the individual events. This Standard defines the phases of El Nino and La Nina using three-month average of Nino-3.4 index. El Nino (La Nina) condition is identified as occurring when the Nino-3.4 values are $\geq 0.5\,^{\circ}C (\leq -0.5\,^{\circ}C)$for at least five months. On this basis, during the years 2005–2015, three El Nino and three La Nina periods were identified (Table 2). As each period covers months from August to December, LD was examined only for these months in this study. The lightning anomalies associated with El Nino and La Nina events were constructed by subtracting the event LD from the August–December climatological mean LD of the 11-year study period (2005–2015).

Table 2
Event periods for the 2005–2015 El Nino and La Nina events (adopted from GB/T 33666-2017) and time periods in this study.

Event	Event periods	Study periods
El Nino	2006.08–2007.01	2006.08–2006.12
	2009.06–2010.04	2009.08–2009.12
	2014.10–2015.12	2015.08–2015.12
La Nina	2007.08–2008.05	2007.08–2007.12
	2010.06–2011.05	2010.08–2010.12
	2011.08–2012.03	2011.08–2011.12

3. Results and discussion

3.1. Spatial distribution

The annual mean LD over the northwest Pacific region for the period 2005–2015 is shown in Fig. 3a. The average annual LD was 3.0 fl km^{-2} yr^{-1} over the entire region, and 90% of the values were < 9.0 fl km^{-2} yr^{-1}. LD varies by at least two orders of magnitude, with the highest densities of > 25 fl km^{-2} yr^{-1} and lowest densities of < 1.0 fl km^{-2} yr^{-1}. The highest values were observed along the coastal areas of southeast Asia and on the MC islands of Malaysia, Indonesia, and the Philippines. The lowest LDs were found in the deep ocean and high-latitude continental areas. The land areas show much higher LDs than the oceanic areas. The annual mean LDs over the designated land areas (areas (1) and (2) in Fig. 1) were 3.3 and 16.5 fl km^{-2} yr^{-1}, respectively, and 2.3 fl km^{-2} yr^{-1} in the open sea (area (4) in Fig. 1). The farther away from the continent, the weaker was the lightning activity over the ocean. Compared with the open sea, lightning occurrence is more frequent in the SCS. LDs in most parts of the SCS were observed around 10–20 fl km^{-2} yr^{-1}, whereas they were < 8.0 fl km^{-2} yr^{-1} in the open sea. The mean LD in the SCS (area (3) in Fig. 1) was 8.9 fl km^{-2} yr^{-1}, which falls in between that of the tropical islands and inland areas. A recent study by Thornton et al. (2017) noticed that lightning activity over oceanic shipping lanes in the SCS was enhanced, due to the emissions of aerosol particles leading to a microphysical enhancement of convection and electrification. The spatial distribution of LD over the northwest Pacific region shown above follows the features of the lightning climatology presented by Christian et al. (2003), Virts et al. (2013b), and Albrecht et al. (2016)

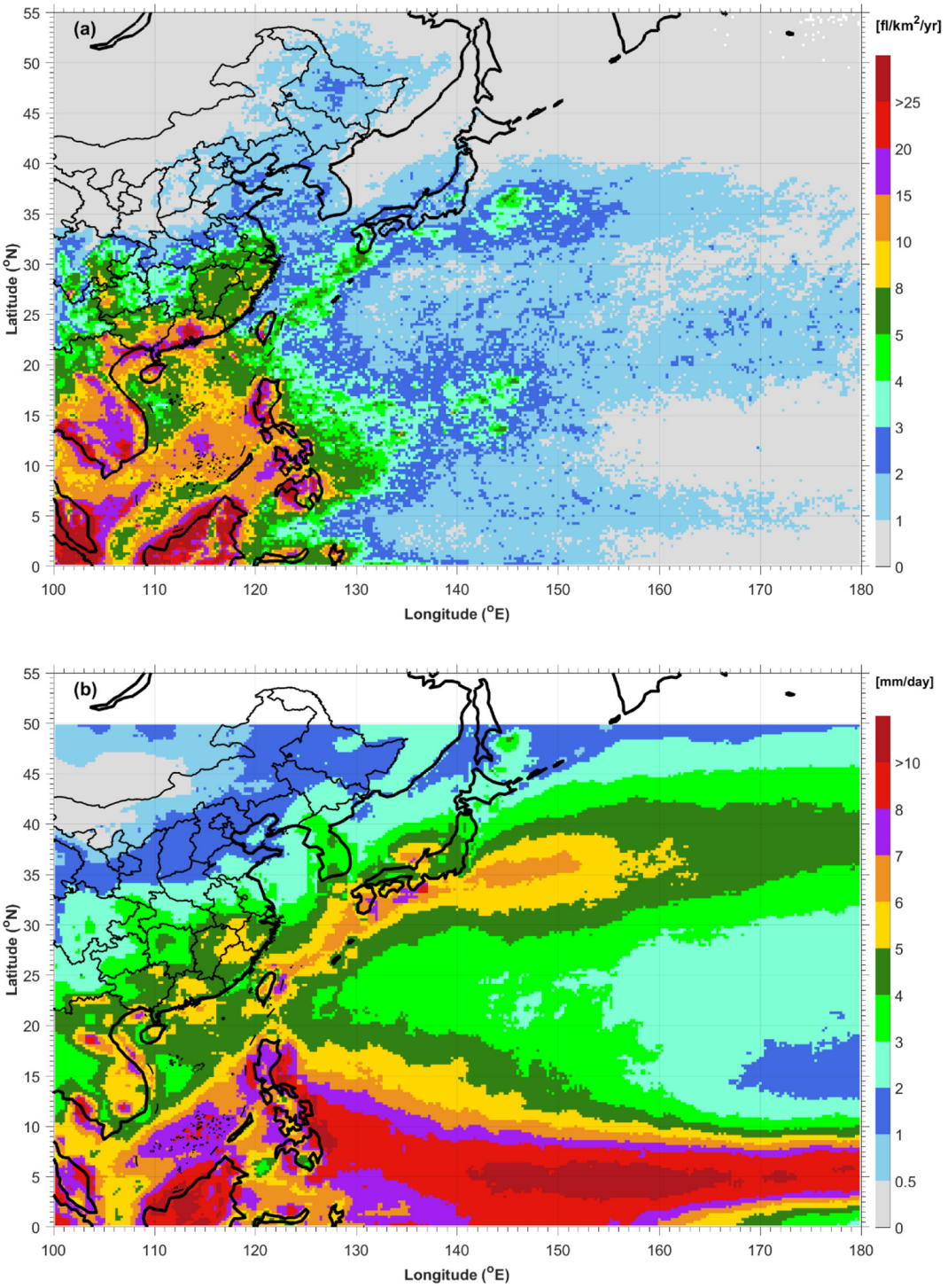

Fig. 3. Distribution of the annual mean (a) adjusted flash density (fl km^{-2} yr^{-1}) and (b) TRMM 3B42 precipitation (mm day^{-1}) over the northwest Pacific region for the period 2005–2015.

using observations from the TRMM LIS.

Fig. 3b shows the geographical distribution of the average daily precipitation derived from TRMM 3B42 during the period 2005–2015. High precipitation rates (> 7 mm day^{-1}) occurred in the area of 0°–10°N and 130°–180°E, corresponding to the rising branch of the Hadley circulation which maintains the Inter Tropical Convergence Zone and the northwest Pacific monsoon. Moderate precipitation (4–7 mm day^{-1}) is located along the coastline from the southern tip of the Indo-China Peninsula extending northward to east of Japan. Low precipitation rates (< 4 mm day^{-1}) are located in the area of 15°–30°N and 130°–180°E, which corresponds with the subsiding branch of the Hadley circulation.

Comparing Fig. 3a with 3b shows that the spatial distribution of areas with a high lightning flash density differs significantly to that of areas with a high precipitation rate. Discharges are not frequent (LD < 4.0 fl km^{-2} yr^{-1}) in the tropical ocean (0°–10°N and 130°–180°E) where a heavy rainfall belt is aligned east–west. Previous studies have noted that convective systems in this region can be characterized as high-precipitation-low-flash (Williams et al., 1992; Zipser, 1994). Warm cloud precipitation processes are characteristic of most of

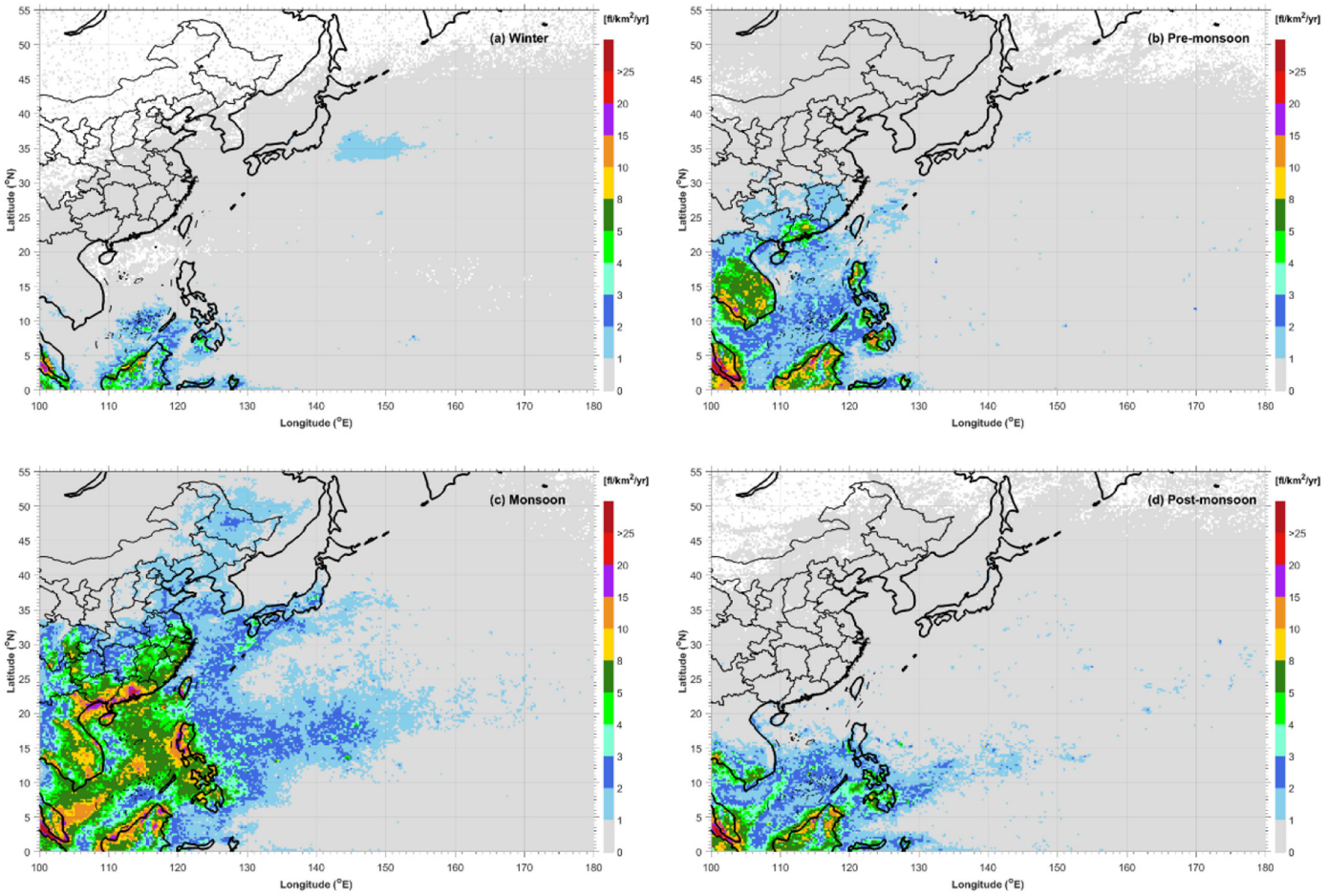

Fig. 4. Seasonal variation of mean lightning density (fl km^{-1} yr^{-1}) during (a) winter season (DJF), (b) pre-monsoon season (MAM), (c) monsoon season (JJAS), and (d) post-monsoon season (ON) averaged for the period 2005–2015.

the storms that develop over the tropical oceans. A large proportion of oceanic precipitation forms below the melting level. Zipser (1994) proposed that a regime of weak and deep rainy clouds is dominant in this area, and that heavy rainfall forms from deep cumulonimbus clouds. Although the cloud top is high, the low convective available potential energy (CAPE) over the oceans restricts vigorous updrafts (Williams et al., 1992). Radar measurements in the vicinity of Darwin, Australia, showed that oceanic convections exhibited radar reflectivity of 10–30 dBZ in the mixed-phase region, compared with the 30–50 dBZ observed in continental convections (Rutledge et al., 1992; Williams et al., 1992). Weak updrafts lead to an insufficient supply of large ice particles and supercooled water in the mixed-phase region, and this reduces electrical activity in the convective systems over the tropical ocean.

3.2. Seasonal variations

Lightning discharge is observed throughout the year in the northwest Pacific region, but shows significant seasonal variations (Fig. 4). During winter season (December–February: DJF; Fig. 4a), the average LD over the entire region reaches its annual minimum. Lightning activity is confined mainly to the tropical islands, including of Malaysia, Indonesia, and the southern Philippines. It is worth noting that in the oceanic area (30°–40°N) east of Japan, LD in winter presents the highest value of the year. This lightning band is associated with wintertime storm tracks. During winter, synoptic-scale cyclones tend to form on the western side of the oceanic currents and propagate eastward, forming the wintertime storm tracks. Vigorous convections and corresponding lightning bands are found along the storm tracks (Virts et al., 2013b). Wintertime lightning in the storm tracks is also observed over the North Pacific Ocean. Based on data from the PacNet Lightning Detection Network, Pessi and Businger (2009) found that most of winter lightning over the North Pacific was associated with clod fronts of midlatitude cyclones. Another associated factor for the oceanic winter lightning east of Japan is the Kuroshio Current. With the WWLLN data, Iwasaki (2014) found there is a high-density lighting area located east of Japan, extending eastwards to the ocean. They pointed out that this oceanic area of high density runs along the Kuroshio Current. Mesoscale disturbances and cloud activities are enhanced under the influence of winter cold-air over the warm sea surface, thus intense disturbances promote active lightning activity over the ocean.

In the pre-monsoon season (March–May: MAM; Fig. 4b), the highest LDs are also located in tropical islands of Malaysia, Indonesia, and the Philippines. However, a sharp increase in LD on the Indo-China Peninsula and in the SCS is also observed. These areas are reported to be the initial onset areas of the Asian summer monsoon. The onset of the monsoon occurs in early- or mid-May (Yuan and Qie, 2008) and is often accompanied by a rapid increase in deep convection. The increasing solar heating during this season leads to instability on land and results in increasing convection there. The wind directions on the Indo-China Peninsula and over the SCS change from northeasterly in winter (Fig. 5a) to westerly/southwesterly in the pre-monsoon season (Fig. 5b). The moist air blown from the Pacific Ocean increases the specific humidity in these areas (Fig. 6b). Convections in the SCS and surrounding landmasses also begin to shift northward from the equator in the pre-monsoon season (Johnson and Ciesielski, 2002). In addition,

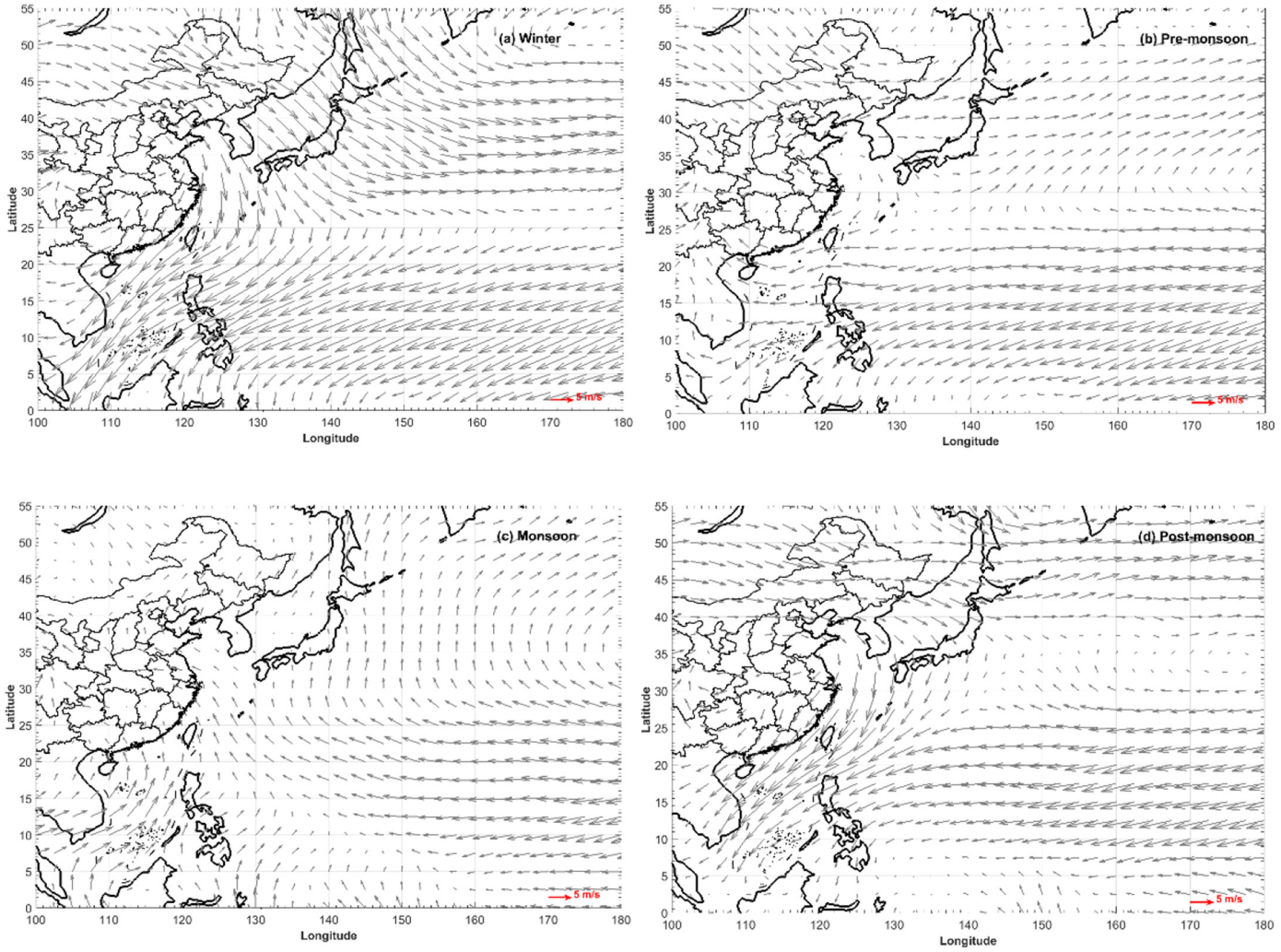

Fig. 5. Seasonal variation of mean surface wind ($m\,s^{-1}$) at 1000 mb pressure level over the northwest Pacific region for the period 2005–2015.

lightning activity varies coherently with the Madden-Julian Oscillation (MJO), which dominates tropical atmospheric variability at intraseasonal time scales. A characteristic feature of the MJO is an area of enhanced precipitation and convention that develops over the Indian Ocean and propagates eastward. The pre-monsoon enhancement in LD on tropical islands over the northwest Pacific region (Fig. 4b) could be influenced by the phase of the MJO. A strong relationship between lighting over the MC and the phase of the MJO has been noted in analyses by Virts et al. (2011).

During the monsoon season (June–September: JJAS; Fig. 4c), the occurrence of active lightning over the mainland extends northward to middle latitudes around 30°N and LDs in the SCS increase sharply. The average LD over the entire region during this season increases to $1.6\,fl\,km^{-2}\,yr^{-1}$, which is 2.4 times that in the pre-monsoon season. The regions of enhanced lightning and convective activity are located mainly in the central and southern SCS and the oceanic area east of the Philippines. With the prevalence of the Asian monsoon, the low-level winds shift from easterly to southwesterly in the SCS. The enhancement of convergence (Fig. 5c) in this area leads to the strengthening of convection in the SCS. The growing southwest monsoon continuously transports abundant water vapor from the Indian Ocean to East Asia (Fig. 6c). Consequently, the monsoon convection gradually extends northwards from the SCS to central and eastern China. Yuan and Qie (2008), using TRMM LIS data, found that the mean flash rate over the SCS is higher during the pre-monsoon season than during the monsoon season. In contrast, our results show that the average LD in this area is highest during the monsoon season. These inconsistent results may be due to the differences between the datasets and definitions of the monsoon period used in the two studies. During the post-monsoon season (October–November: ON; Fig. 4d), electrical activity decreases sharply in middle latitudes and is concentrated mainly along the tropical coastlines and in the southern SCS.

3.3. Monthly variations

The monthly percentage of lightning strokes over the northwest Pacific region for the period 2005–2015 is presented in Fig. 7, as well as the variations in the monthly precipitation rate. The percentage is the ratio of the number of lighting (precipitation amount) in that month to the annual mean number of lightning (precipitation amount) over the northwest Pacific region. The main thunderstorm season begins in May and lasts until October. These active months generate about 72.9% of all lightning strokes over the study period. Lightning activity peaks in August, when 13.9% of all lightning occurs. The percentage begins to decline significantly in November and remains low (< 7%) from December to April. The weakest month for lightning activity is February (2%). The distribution of monthly lightning is correlated with the variation in monthly precipitation (Fig. 7), which is characterized by a low rate from December to April in the winter and early pre-monsoon season, and a high rate from July to September in the monsoon season.

Fig. 8 shows the average monthly variations in LD over the northwest Pacific region over the period 2005–2015. The figures show a

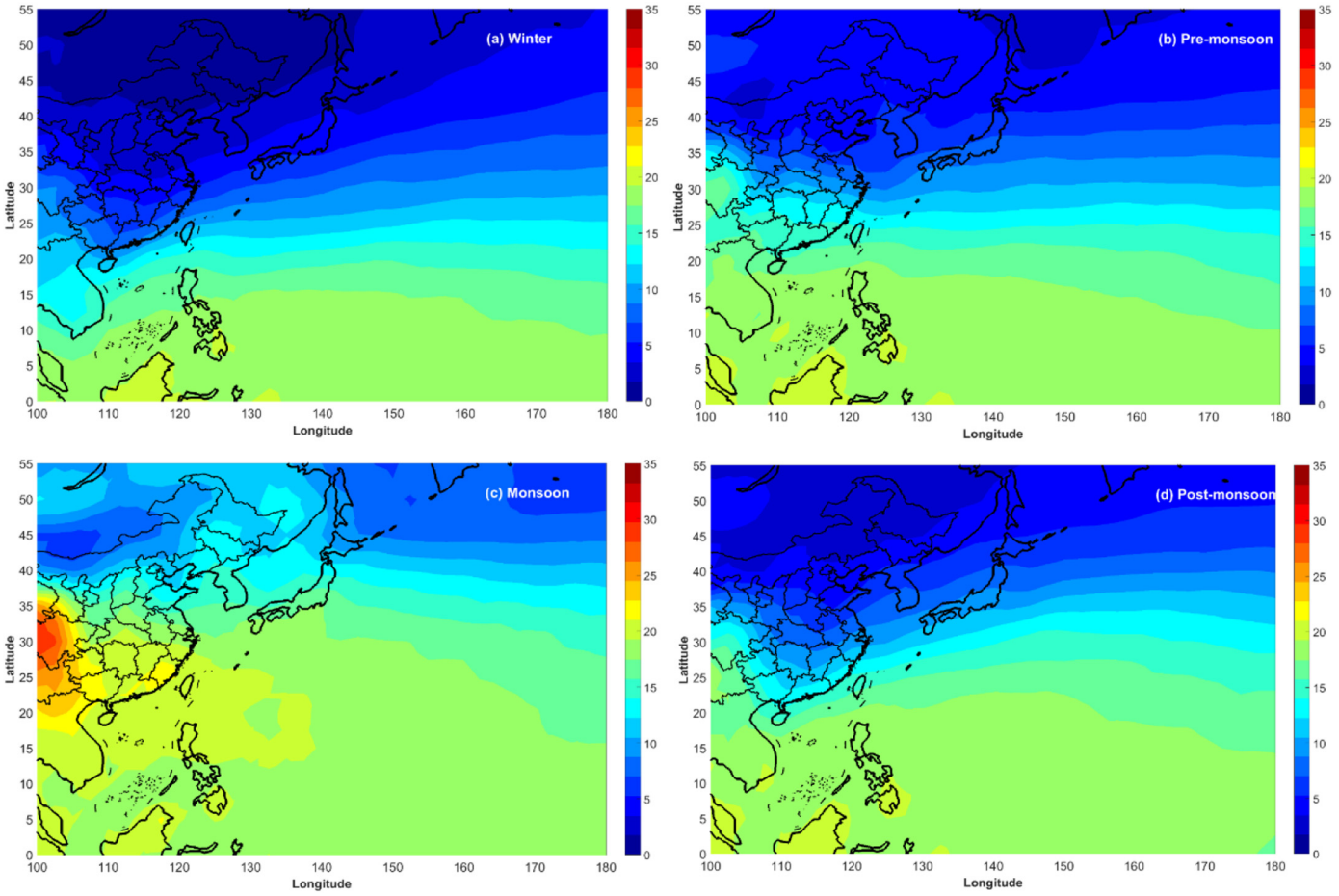

Fig. 6. Seasonal variation of mean specific humidity ($g\,kg^{-1}$) at 1000 mb pressure level over the northwest Pacific region for the period 2005–2015.

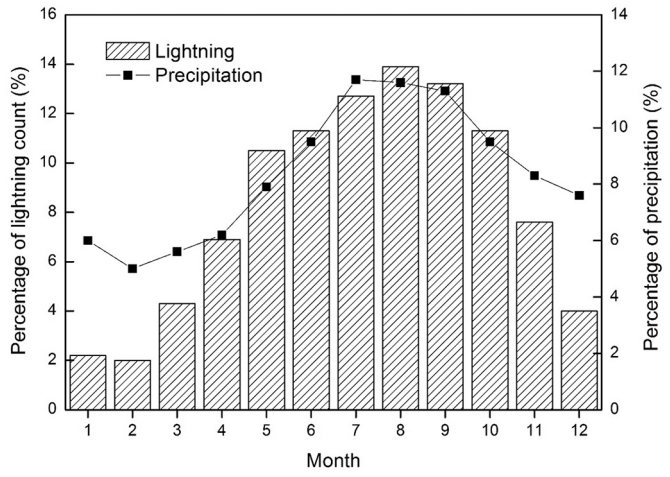

Fig. 7. Monthly variation of lightning and precipitation over the northwest Pacific region for the period 2005–2015, expressed as the percentage of the lightning count and precipitation amounts for each month.

well-defined thunderstorm season extending from May to October as indicated in Fig. 7. LD values over the whole region are low in January and February (Fig. 8a and b). The LD begins to increase in March, and high values are confined mainly to the tropical islands. It is worth noting that there is a sharp increase in LD in the Strait of Malacha (Fig. 8c) in March. The areas of active lightning expand northwards to the Indo-China Peninsula from April and LD in the domain gradually increases (Fig. 8d). The lightning activity over the SCS also appears to increase in April, which is consistent with the results of Yuan and Qie (2008). May is considered to be the onset month of the Asian summer monsoon, and its initial onset occurs over the SCS (Johnson and Ciesielski, 2002). The outbreak of the monsoon strengthens the convection over the SCS and its surrounding land masses. This is also indicated by the increased LD there in Fig. 8e.

June is the most active month for lightning in the SCS and is when the LD over the sea area reaches its annual maximum. The areas of highest LD and intense convection appear to shift northwards from the tropical islands, jumping across the SCS to southern China (typically Guangdong Province; Fig. 8f). The arrival of the convection there marks the beginning of the Meiyu rainy season (Xu et al., 2009). The convections move further north in July and August, when lightning over the land areas reaches its northernmost extent and increased lightning activity is observed over central China and Japan (Fig. 8g and h). However, LDs there are not as high as in southern China in June. Additionally, lightning activity over the deep ocean is strongest in August. In September (Fig. 8i), the strong monsoon convection weakens and the areas with high LD contract quickly southwards. October (Fig. 8j) is found to have intense lightning activity in islands and coastal areas in the tropics. During November and December (Fig. 8k and l), most of the northwest Pacific region enters a period of greatly reduced thunderstorm activity, whereas the MC islands still show persistent lightning activity in the winter months.

3.4. Diurnal variations

The diurnal cycle is one of the fundamental modes of variability within the climate system. Fig. 9 shows the diurnal distributions of electrical activity in our four study areas; i.e., inland, tropical islands,

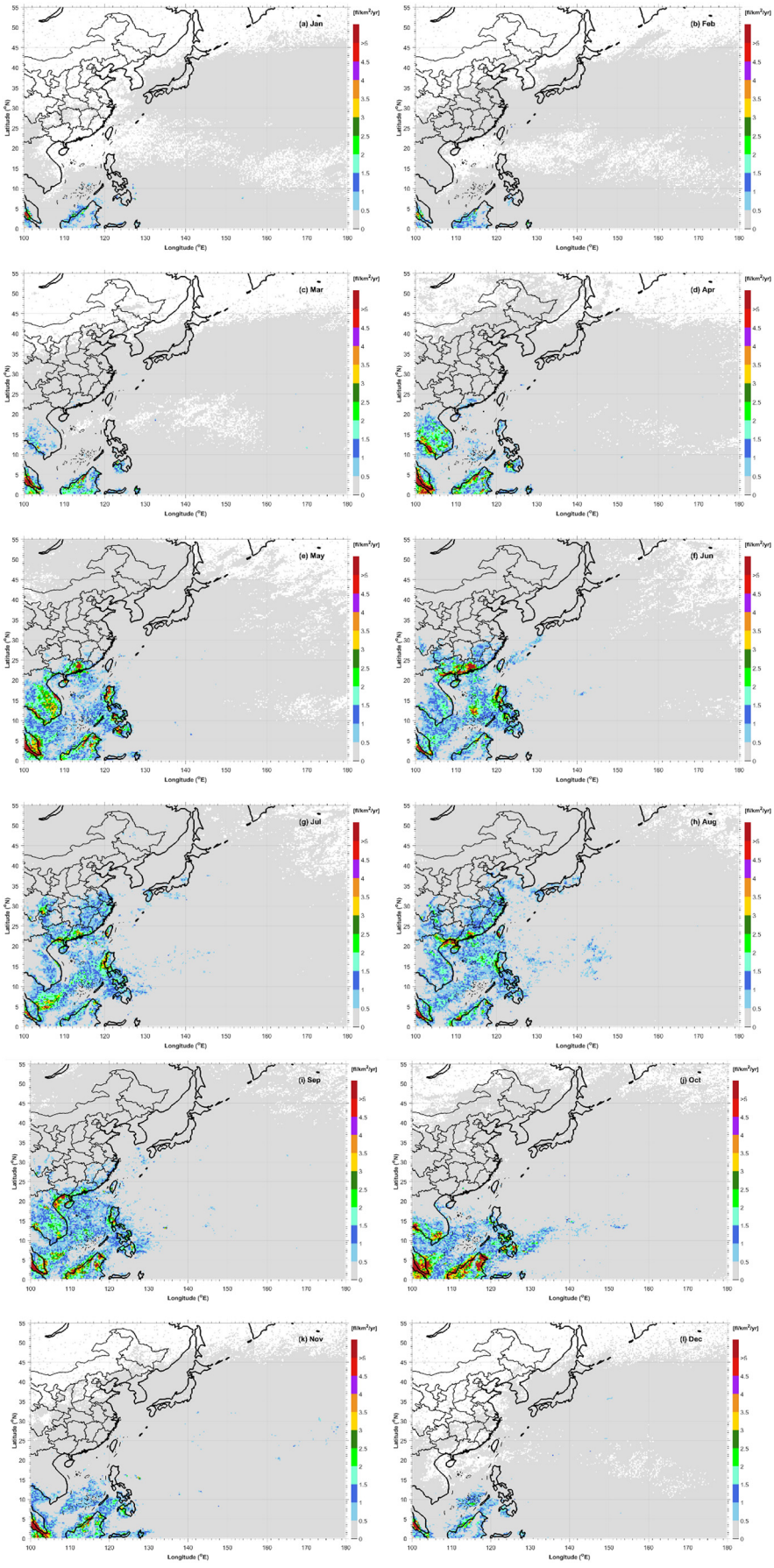

Fig. 8. Monthly variations of lightning density over the northwest Pacific region for the period 2005–2015.

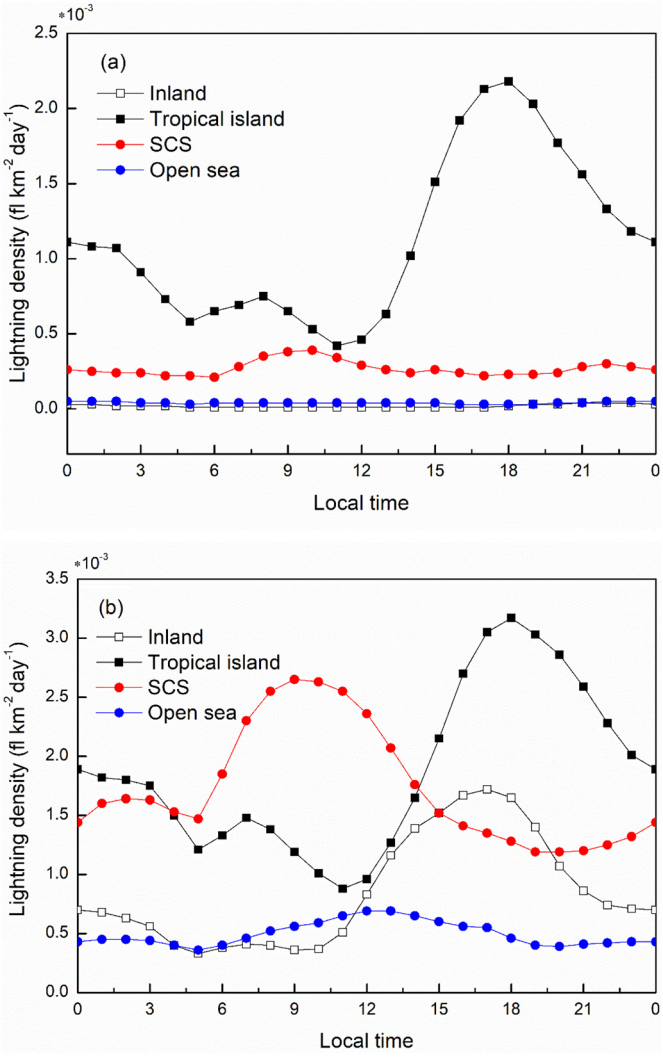

Fig. 9. Diurnal variations of lighting density (fl km^{-2} day^{-1}) over the inland, tropical islands, the South China Sea (SCS), and the open sea areas indicated in Fig. 1 in (a) winter (December to February) and (b) monsoon (June to September) seasons for the period 2005–2015.

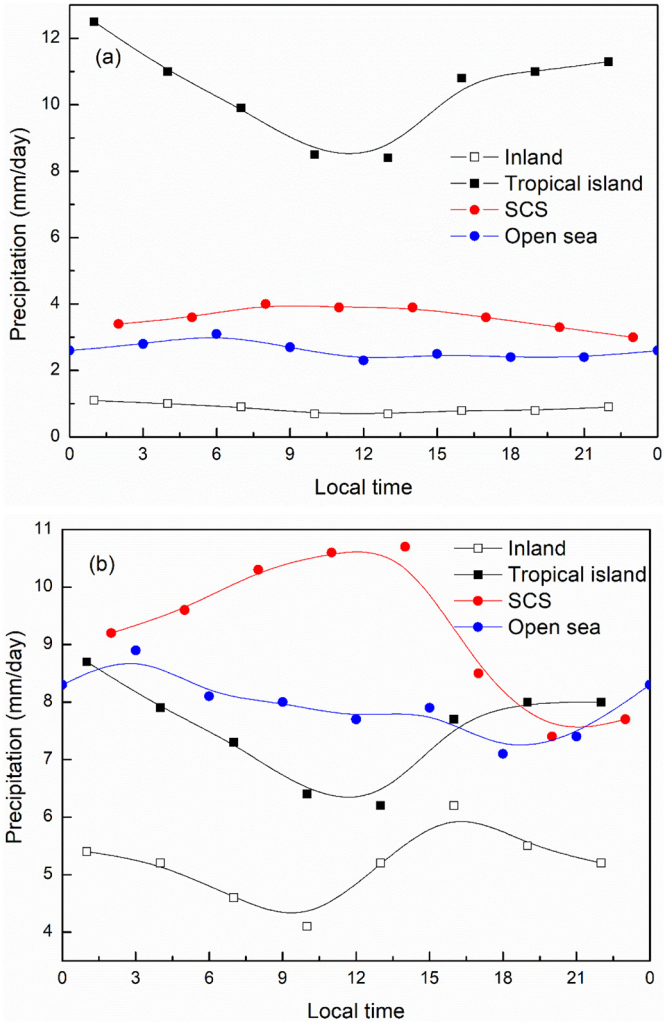

Fig. 10. As Fig. 9 but for TRMM precipitation rate (mm day^{-1}). Curves are fitted by splining points from the 3-h TRMM 3B42 precipitation data.

the SCS, and the open sea (Fig. 1), for the winter and monsoon seasons. Fig. 10 shows those for the precipitation rates from TRMM 3B42. During the winter season (Fig. 9a), the lowest LDs are observed inland and over the open sea, with hourly LD values < 1 X 10^{-5} fl km^{-2} day^{-1}. LDs over the tropical islands are the largest among the four designated areas. LDs in the SCS are larger than that of inland and the open sea, but smaller than that of the tropical islands. Similar characteristics are also found in the diurnal cycles of precipitation in the same season (Fig. 10a). The diurnal variations of lightning activity become more obvious during the monsoon season (Fig. 9b). The average LDs over the tropical islands remain the largest among the four areas. Meanwhile, lightning activity is significantly increased inland and over the SCS during the monsoon season. Strong convection over the SCS during this season is also evident in the diurnal precipitation patterns (Fig. 10b), which reveals that hourly precipitation rates in the SCS are the largest among the four areas. LD values in the open sea still remain the lowest among the four areas, but are higher compared with those in the winter season and feature a peak at noon (1200 LT). However, the daily precipitation rates in the open sea are only lower than that in the SCS and rank the second among the four areas. This is due to the differences of regimes between the precipitation and lightning in the tropical ocean and is consistent with the results in Section 3.1.

The diurnal distribution of lightning shows remarkable differences over the land and ocean. Inland and over the MC islands, an evident peak occurs in the late afternoon between 1700 and 1800 LT during the monsoon season (Fig. 9b), with LD values of 1.7×10^{-3} fl km^{-2} day^{-1} and 3.2×10^{-3} fl km^{-2} day^{-1}, respectively. The minimum lightning activity inland and over the MC islands occurs between 1100 and 1200 LT with LDs of 0.36×10^{-3} fl km^{-2} day^{-1} and 1.0×10^{-3} fl km^{-2} day^{-1}, respectively. Thus, LD over the land areas at noon is roughly 3–4 times less than that during the late afternoon. These features of the lightning distribution over land are consistent with lightning over the continental United States (Holle, 2014) and Southern China (Zheng et al., 2016). Strong diurnal variations in lightning and precipitation are observed over the MC islands (Figs. 9b and 10b). Due to the smaller heat capacity of land compared to that of the ocean, the local temperature and pressure gradients result in sea breezes in daytime and land breezes at night. Land-sea breeze is an important factor in the hydrological cycle of the MC (Hidayat and Ishii, 1998; Yang and Slingo, 2001) and may be the main cause of the diurnal variations in lightning activity around these regions. Convections over the MC begin to develop around noon. As the sea-breeze fronts propagate inland and intensify during the afternoon, lightning activity is enhanced with peak frequency around 1800 LT. Lightning activity could persist into midnight and last to early morning. These afternoon maxima in lightning and convection have also been observed previously

on the MC islands of Borneo (Yang and Slingo, 2001), Sumatra (Virts et al., 2013b) and Java (Hidayat and Ishii, 1998). Similar behavior has also been noted in the diurnal cycle of precipitation over MC islands by Mori et al. (2004) and Qian (2008).

In contrast to the strong diurnal variations over the continent, the diurnal distribution of lightning over the open sea is evenly distributed throughout the day and night. During the monsoon season, the maximum LD over the open sea occurs around noon and no minimum is observed (Fig. 9b). The distribution of lightning over the open sea in the northwest Pacific is consistent with global oceanic lightning activity (e.g., Zipser et al., 2006; Lay et al., 2007), which displays a much smaller diurnal lightning variation and a slightly enhanced LD over the morning to noon hours. Different mechanisms of convection lead to the significant differences in the diurnal cycle of lightning between the land and the open sea. The diurnal afternoon maximum on land is linked to boundary layer instability caused by daytime heating. Conversely, the oceanic maximum is associated with radiative heating and longwave cooling, as well as enhanced nocturnal mesoscale convective systems (Nesbitt and Zipser, 2003).

Lightning activity in the SCS is much stronger (i.e., LD about 4 times greater) than that in the open sea (Fig. 9). Unlike the flat variations over the open sea, LDs over the SCS show an obvious peak in the morning (0900 LT). It is interesting that the maximum LD over the SCS is 3 h ahead of the maximum over the open sea (1200 LT). These variations in the peak time of lightning between the two regions may be caused by the complex coastal topography surrounding the SCS. The diurnal convection in the SCS differs from the convective pattern over the open ocean (Aves and Johnson, 2008). Moreover, the SCS is near the continent. Coastline effects and gravity wave forcing by the nearby continent (Yang and Slingo, 2001) could influence the diurnal cycles in the SCS. The study of Aves and Johnson (2008) suggested an increase in the diurnal phase of maximum convection with increasing distance from the coast in the SCS. They defined this as a “propagation signal”. This phenomenon has also been observed in the diurnal variations in convection and precipitation over the Bay of Bengal (Yang and Slingo, 2001).

3.5. Contribution of tropical cyclones to lightning activity

Fig. 11a shows the distribution of annual mean LD produced by TCs over the northwest Pacific region during the period 2005–2015. The best-tracks of the storms are presented in Fig. 2. TC lightning occurs mainly in the area bounded by 10°–25°N, 107°–103°E. Two maximum areas ($> 2.0\,\mathrm{fl\,km^{-2}\,yr^{-1}}$) of TC LD are observed: 1) east of the Philippines; and 2) the coastline and offshore areas of south China. This indicates that lightning activity is enhanced when the storms are approaching landfall. The spatial distribution of TC lightning is consistent with the distribution of the TC paths and intensity (Fig. 2). Lightning flash density begins to increase when the storms are approaching the Philippines. After making landfall on the Philippines, the activity of TC lightning weakens. Lightning activity is enhanced again when the storms cross the Philippines and enter the SCS. Thus, it is inferred that some storms re-intensify in the SCS. LD reaches a maximum during the pre-landfall periods over China and then reduces sharply after landfall. Some storms undergo a transition to extratropical cyclones and have tracks that extend to high latitudes where LDs generated by TCs are very low.

The contribution of TC lightning to total lightning over the northwest Pacific region is quantified in Fig. 11b. The average contribution rate of TC lightning in the domain is 2.2%, with 80% of the samples below 3%. There are two areas of significant contribution, namely, the oceanic area east of the Philippines and the offshore area southwest of Taiwan island. Note that the contribution rate is not the highest in the area of the maximum TC LD; i.e., the southeast coastal area of China. This indicates that, in these areas, other local synoptic-scale systems generate a larger proportion of lightning than do TCs. In contrast, the proportion of TC lightning can exceed 75% over some oceanic regions far from land. The distribution of the zonally averaged LD for the northwest Pacific region and for TCs are shown in Fig. 12. The total LD over the entire region decreases with increasing latitude. The TC LD shows a unimodal distribution with latitude, with the peak appearing at 14°–22°N. In this latitude zone, the average TC LD is $0.3–0.4\,\mathrm{fl\,km^{-2}\,yr^{-1}}$. The distribution of maximum contribution rate is consistent with the peak in TC LD, but within a smaller latitude zone of 13°–20°N.

3.6. Lightning anomalies associated with El Nino and La Nina events

Using the WWLLN data, the magnitude of the variation in LD associated with El Nino and La Nina events was investigated. The average LD during El Nino events increases by 10.3%, whereas during La Nina events it decreases by 4.8%, when compared with the average LD during the study period of 2005–2015 in the domain. Fig. 13 gives the distribution of lightning anomalies for the events during the study period (2005–2015). During the El Nino period (Fig. 13a), lightning activity is abnormal in three latitude belts: 1) in the 0°–10°N tropical region, more lightning is found in the coastal areas of the MC islands, Strait of Malacca, southern SCS, and oceanic areas east of the Philippines; 2) in the 10°–25°N subtropical region, lightning activity in the central and northern SCS is weaker during the El Nino events; and 3) in the 25°–40°N extratropical region, more lightning than normal is found in the East China Sea between Taiwan island and Japan.

The increased LDs in the coastal areas of the MC islands are caused by the enhanced surface air temperature over the tropical islands and the strong land-sea breeze circulations during El Nino (Hamid et al., 2001). The increased surface air temperature over the islands may cause larger CAPE, deeper clouds and larger updrafts in convection. For example, stronger storm intensity was observed over Indonesia during the 1997–98 El Nino event, which was indicated by the higher cloud tops and thicker zones containing ice phase precipitation (Hamid et al., 2001). Another mechanism that possibly affects the larger LDs in the coastal areas during El Nino are land-sea breeze circulations. As the SST is suppressed over the western Pacific Ocean and the surface air temperature over the islands increases, the land-ocean contrast is more significant and deeper convection may occur within the tropical islands. This deeper convection may cause greater updrafts, which could in turn generate the larger LD values. One of the reasons that lightning increases in the oceanic areas east of the Philippines is probably the increased number and intensity of TCs that develop in the northwest Pacific and move toward the Philippines. ENSO events have shown vital impacts on variations in TC activity over the northwest Pacific (Wang and Chan, 2002). An example of the good agreement between El Nino events and cyclogenesis is evident in a study from the Gulf of Mexico Basin by Goodman et al. (2000), who found enhanced upper-level jet stream winds produced increased TCs and cyclogenesis and thus an environment favorable for lightning within this region. Similarly, Kumar and Kamra (2012) found a 30% increase of cyclonic storms in the 1998 El Nino year compared with the average number for other years in the Indian Ocean. Previous studies also found that there is a tendency for the El Nino periods to show more intense and longer-lived TCs than the La Nina periods (Camargo and Sobel, 2005).

A distinct distribution of lightning anomalies is shown for the 2005–2015 La Nina periods (Fig. 13b). In the 0°–10°N tropical region, negative anomalies dominate in coastal areas of tropical islands, where enhanced lightning occurs during the El Nino years. Large positive anomalies are apparent in the 10°–25°N latitude belt; i.e., the western coastal areas of the Philippines and the central and northern SCS. Enhanced lightning activity in these regions was also observed during the 1993–2005 La Nina events by Satori et al. (2009); see their Fig. 5), whereas lightning in these areas was normal during the El Nino events over the same period. Additionally, a northward shift of enhanced lightning activity in the 25°–40°N latitude belt is shown (Fig. 13b).

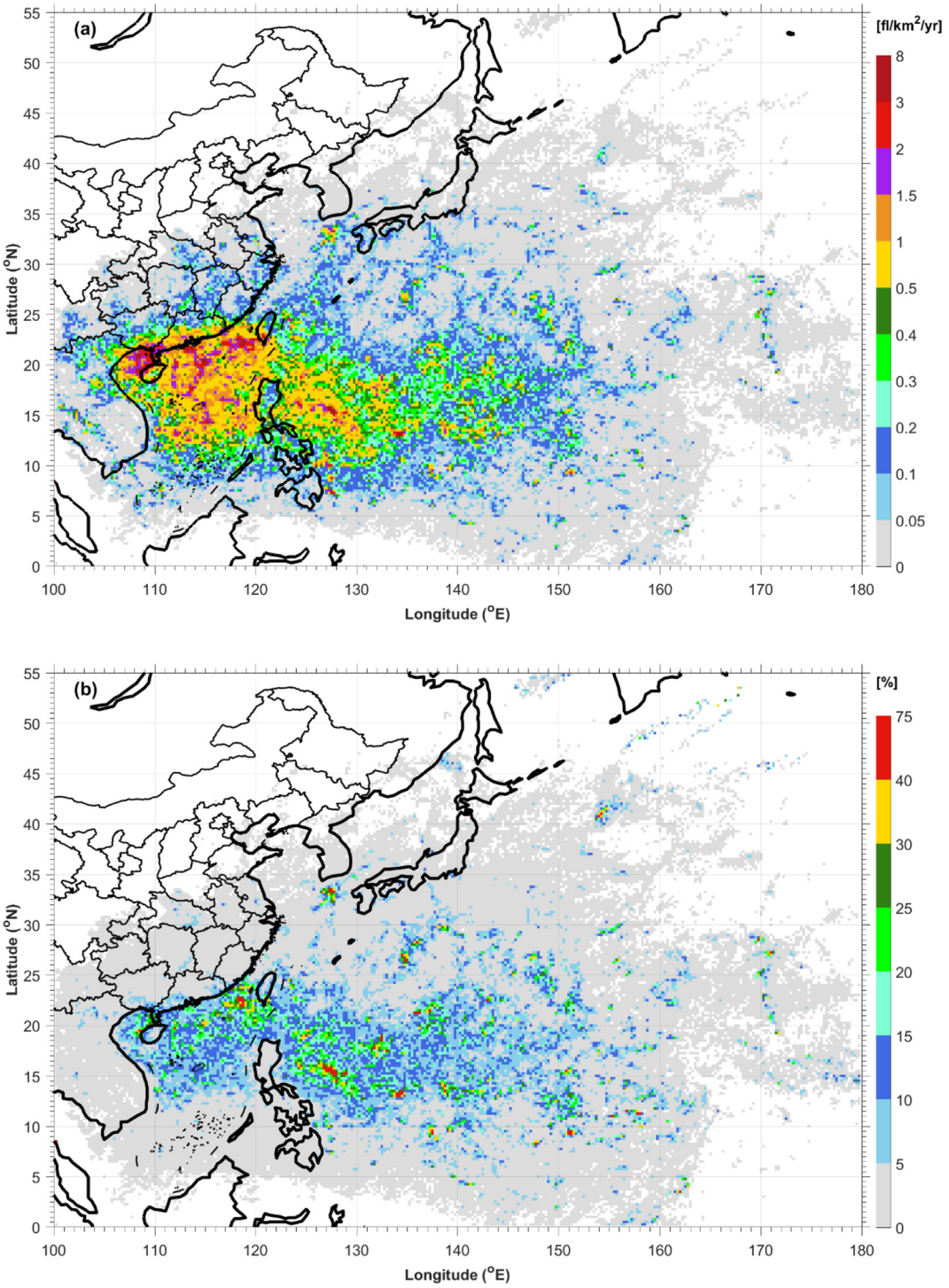

Fig. 11. Distribution of the annual mean (a) lightning density (fl km^{-2} yr^{-1}) and (b) lightning contribution rate (%) for tropical cyclones over the northwest Pacific region for the period 2005–2015.

Positive anomalies shift from the East China Sea during El Nino periods to the Yellow Sea (30°–40°N, 120°–130°E) in the La Nina periods.

The activity of convection and lightning over the SCS is sensitive to ENSO events. Positive anomalies move from the southern SCS in El Nino periods to the central and northern SCS in La Nina periods. This shift is consistent with the results of Satori et al. (2009) that were based on Schumann resonance and LIS data. Fig. 14 gives the anomalies of the surface wind vectors from the NCEP–NCAR reanalysis dataset. During the El Nino periods, in the southern SCS, the wind vectors from the sea to the MC islands (i.e., Malaysia and Indonesia) are remarkable (Fig. 14a). As a result, the moist air from the sea generates strong convection and intense lightning activity along the coastline of the islands. In contrast, during the La Nina period, the wind direction is from the land to the sea, causing negative anomalies in the lightning activity there. During the La Nina periods, there is an increase in winds blowing from the surrounding land into the SCS, which causes a convergence of wind vectors in the central and northern SCS (Fig. 14b). Therefore, increased updrafts and convective activity develop over this region and generate positive anomalies in the lightning activity during the La Nina periods.

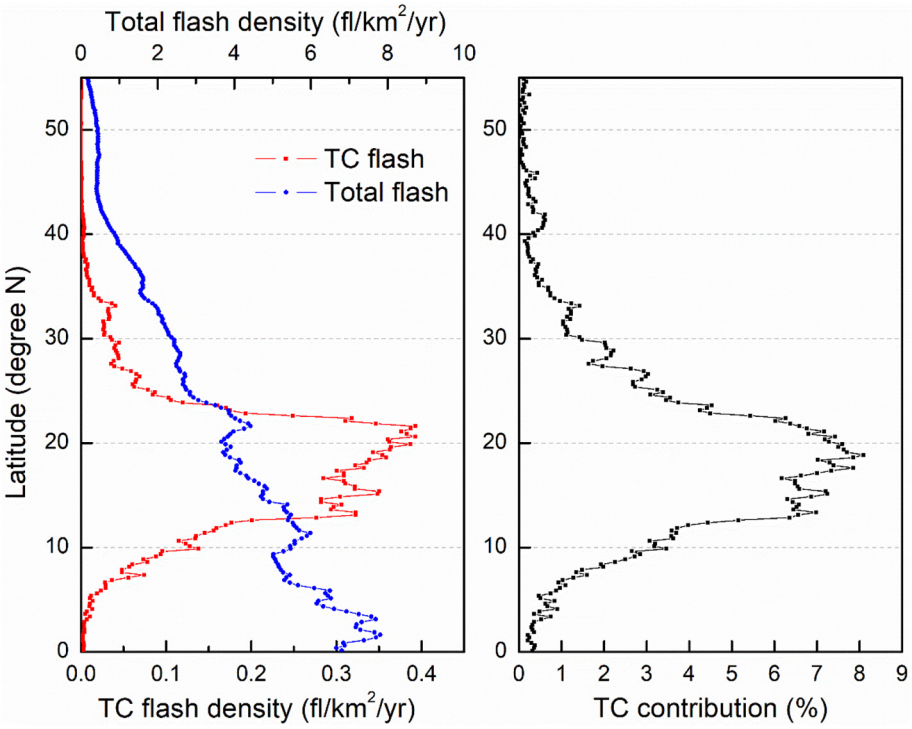

Fig. 12. Distribution of zonally mean values for total lightning density over the northwest Pacific region (blue line), TC lightning density (red line), and TC lightning contribution rate (black line). (For interpretation of the references to colour in this figure legend, the reader is referred to the web version of this article.)

4. Conclusions

In this paper, we have investigated the climatology of the spatial and temporal variability of lightning activity over the northwest Pacific region (0°–55°N, 100°–180°E) by analyzing data for the period 2005–2015 obtained from the WWLLN. We also investigated the contribution of TCs to the climatological lightning, and the impacts of El Nino and La Nina events on lightning distribution over this region. The DE of the WWLLN was not homogenous during the period of study; consequently, we used the LIS/OTD climatology data to adjust for the increased DE of the WWLLN. Our main conclusions are presented below.

1) The spatial distribution of lightning activity over the northwest Pacific region showed that the mean LD over the study period was 3.0 fl km^{-2} yr^{-1}. The highest densities were located along the coastal areas of southeast Asia and tropical islands, and the lowest LDs occurred over the deep ocean and high-latitude continental areas. The land areas showed much higher LDs than oceanic areas, except for the SCS. The distribution of high-LD areas differed significantly from areas with high precipitation rates. The tropical ocean was characterized by high precipitation rates but low lightning flash densities, which is consistent with previous studies.
2) Significant seasonal variations in lightning discharge were observed over the northwest Pacific region. The average LD in the region reached a minimum in winter (DJF), especially in the deep ocean. However, in the oceanic area (30°–40°N, 140°–155°E) east of Japan, the highest LD values occurred in winter. A sharp increase in LD on the Indo-China Peninsula and in the SCS, the initial onset areas of Asian monsoon, was observed during the pre-monsoon season (MAM), with the wind directions in these areas changing from northeasterly in winter to westerly/southwesterly in the pre-monsoon season. In the monsoon season, the enhanced regions of lightning and convective activity were located mainly in the central and southern SCS and the oceanic area east of the Philippines. The monthly variations in lightning activity showed an obvious thunderstorm season during July, August and September, which was consistent with the peak months for the precipitation rate. The lowest month for both lightning activity and precipitation rate was February.
3) The diurnal variations in lightning activity in the four areas studied were compared. LDs in the open sea remained the lowest and had flat diurnal variations. The diurnal cycles of lightning inland and over the tropical islands differed remarkably from the ocean. On land, lightning activity showed an evident peak in the late afternoon (1700–1800 LT). Unlike the flat variations over the open sea, lightning activity in the SCS was much stronger and showed an obvious peak in the morning (0900 LT). The maximum LD over the SCS was 3 h ahead of the maximum in the open sea. This may be due to geographic effects, local weather patterns, coastline effects, and the gravity wave effect of the nearby continent.
4) TC lightning activity over the northwest Pacific region occurred mainly in the area of 10°–25°N and 107°–103°E, and showed a unimodal latitudinal distribution that peaked around 14°–22°N. Two maximums of TC LD were observed, one located east of the Philippines and the other along the coastline and offshore from south China, indicating that enhanced lightning activity is produced by storms that are approaching landfall. Two areas that contributed a large proportion of TC lightning were the oceanic area east of the Philippines and the offshore southwest of Taiwan.
5) Lightning variations associated with the 2005–2015 El Nino and La Nina events were also investigated. Compared with the average LD over the whole period, the average LD during the El Nino events increased by 10.3%, whereas during the La Nina events it decreased by 4.8%. Two distinct regions were found to have more lightning during the El Nino events: 1) the coastal areas of the MC islands, Strait of Malacca, southern SCS, and oceanic areas east of the Philippines in the 0°–10°N tropical region; and 2) the East China Sea between Taiwan island and Japan in the 25°–40°N extratropical region. We propose that the increased LDs in these areas were caused by the enhanced synoptic-scale forcing, strong land-sea breeze circulations, and the increased number and intensity of

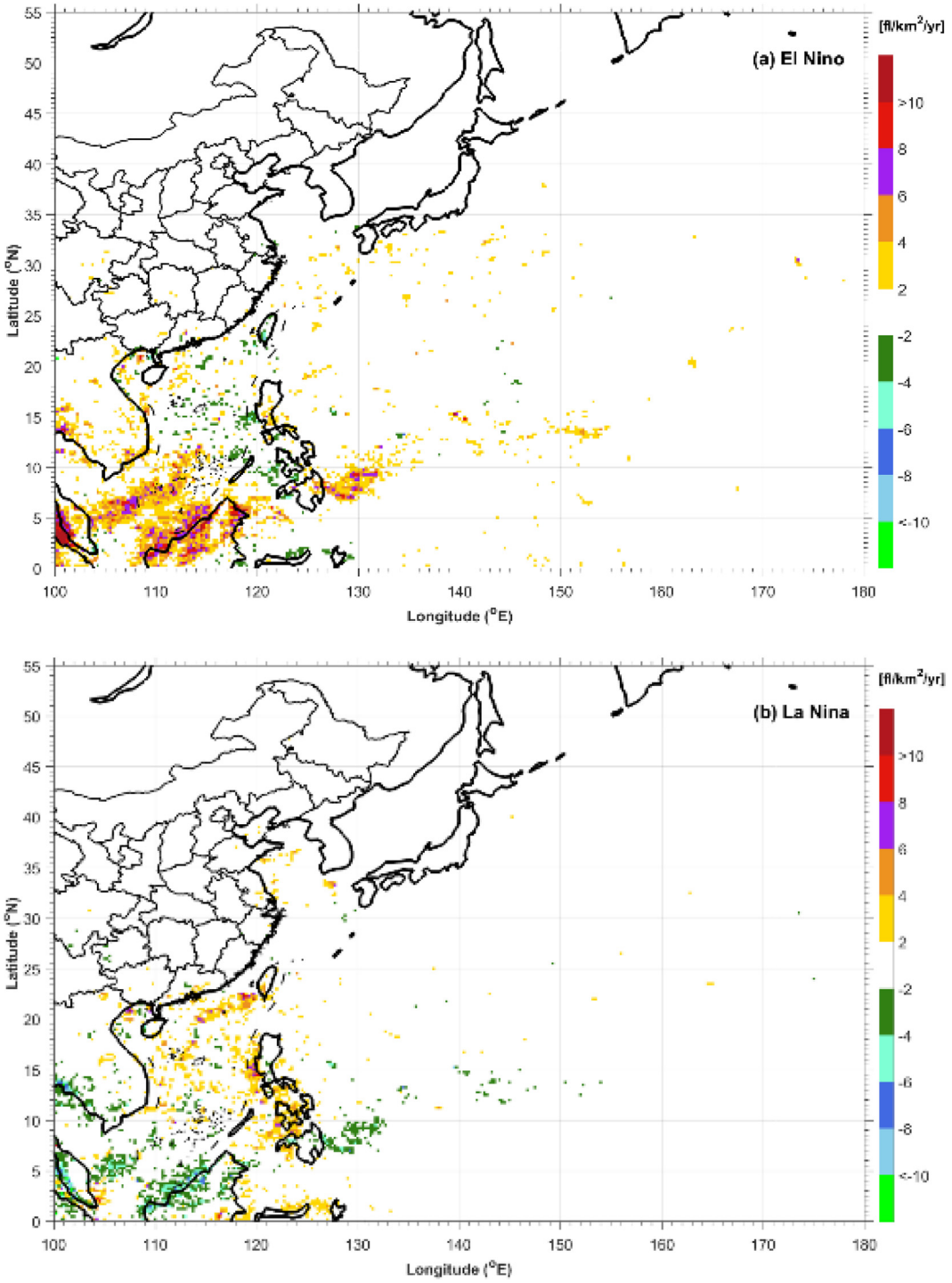

Fig. 13. Lightning density anomaly for (a) El Nino and (b) La Nina events for the period 2005–2015.

tropical storms that developed in the northwest Pacific and moved toward the Philippines. In contrast, during the La Nina periods, large positive LD anomalies presented in the western coastal areas of the Philippines and the central and northern SCS. A northward shift of the enhanced lightning activity in the SCS was observed during the La Nina periods. The positive anomalies are associated with the convergence of wind vectors in the central and northern SCS.

Acknowledgments

The authors thank the editor and two anonymous reviewers for their helpful comments and suggestions. This work was supported by the National Natural Science Foundation of China (Grant 41405004), the National Basic Research and Development Program of China (Grant 2014CB441406), the Basic Research Fund of Chinese Academy of Meteorological Sciences (Grant 2016Z002), the National Key Research and Development Program of China (Grant 2017YFC1501502), and the Support Program for the Returned Overseas Scholars. Lightning data were provided by the World Wide Lightning Location Network (http://wwlln.net), a collaboration among over 50 universities and institutions. Best-track data were obtained from the Shanghai Typhoon Institute (http://tcdata.typhoon.gov.cn/en/). TRMM LIS/OTD climatology data

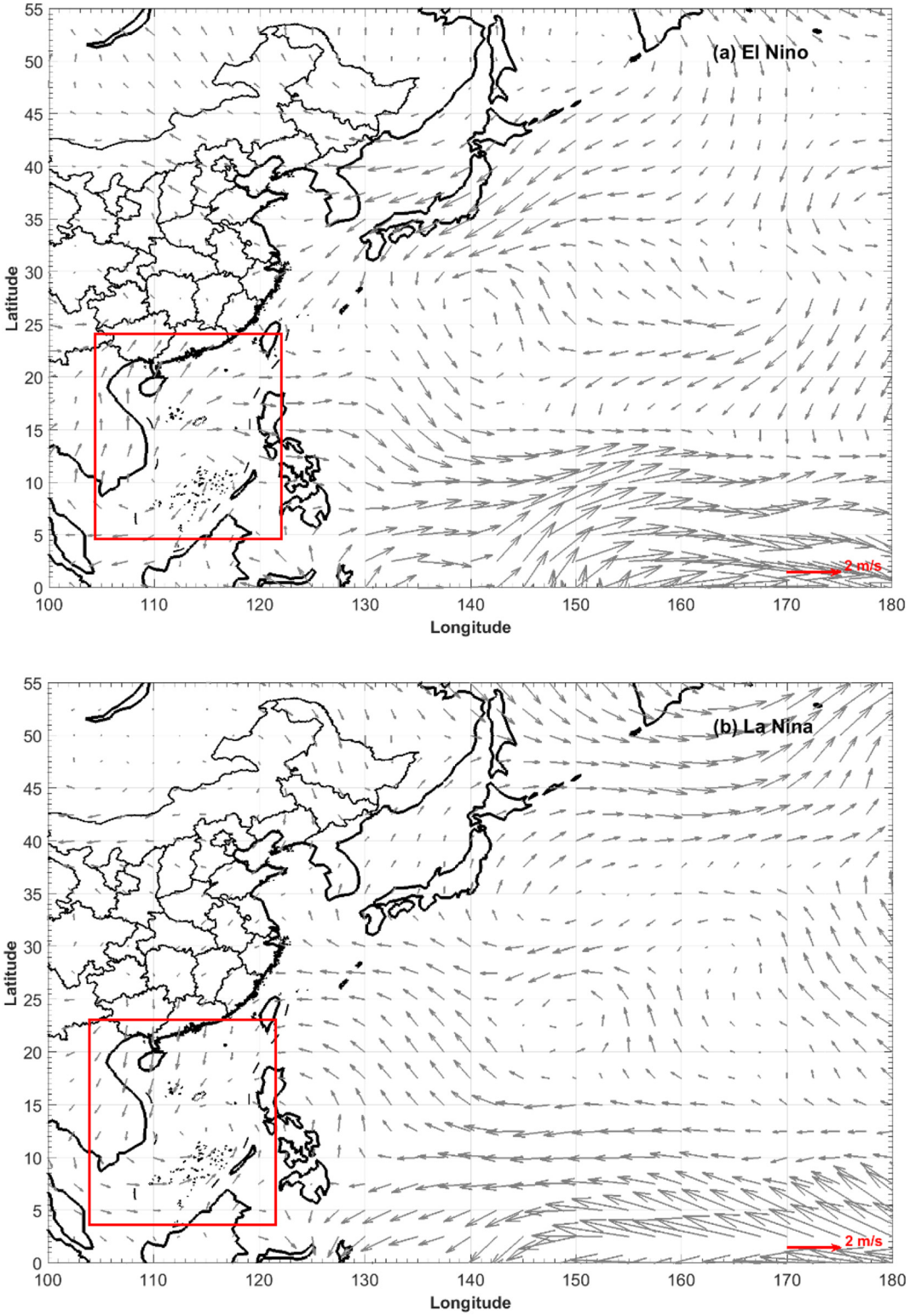

Fig. 14. Anomaly of surface wind ($m\,s^{-1}$) at 1000 mb pressure level for the (a) El Nino and (b) La Nina events for the period 2005–2015.

were obtained from the Global Hydrology Resource Center (http://lightning.nsstc.nasa.gov/data/).

References

Abarca, S.F., Corbosiero, K.L., Galarneau Jr., T.J., 2010. An evaluation of the Worldwide Lightning Location Network (WWLLN) using the National Lightning Detection Network (NLDN) as ground truth. J. Geophys. Res. 115, D18206. http://dx.doi.org/10.1029/2009JD013411.

Abarca, S.F., Corbosiero, K.L., Vollaro, D., 2011. The World Wide Lightning Location Network and convective activity in tropical cyclones. Mon. Weather Rev. 139, 175–191.

Albrecht, R.I., Goodman, S.J., Buechler, D.E., Blakeslee, R.J., Christian, H.J., 2016. Where are the lightning hotspots on earth? Bull. Am. Meteorol. Soc. 97, 2051–2068.

Altaratz, O., Levin, Z., Yair, Y., Ziv, B., 2003. Lightning activity over land and sea on the eastern coast of the Mediterranean. Mon. Weather Rev. 131, 2060–2070.

Aves, S.L., Johnson, R.H., 2008. The diurnal cycle of convection over the northern South China Sea. J. Meteorol. Soc. Jpn. 86, 919–934.

Black, R.A., Hallett, J., 1986. Observations of the distribution of ice in hurricanes. J. Atmos. Sci. 43, 802–822.
Bovalo, C., Barthe, C., Begue, N., 2012. A lightning climatology of the South-West Indian Ocean. Nat. Hazards Earth Syst. Sci. 12, 2659–2670.
Bovalo, C., Barthe, C., Yu, N., Bègue, N., 2014. Lightning activity within tropical cyclones in the South West Indian Ocean. J. Geophys. Res. Atmos. 119, 8231–8244.
Camargo, S.J., Sobel, A.H., 2005. Western north Pacific tropical cyclone intensity and ENSO. J. Clim. 18, 2996–3006.
Cecil, D.J., Buechler, D.E., Blakeslee, R.J., 2015. TRMM LIS climatology of thunderstorm occurrence and conditional lightning flash rates. J. Clim. 28, 6536–6547.
Christian, H.J., et al., 2003. Global frequency and distribution of lightning as observed from space by the optical transient detector. J. Geophys. Res. 108, 4005. http://dx.doi.org/10.1029/2002JD002347.
Curtis, S., Adler, R.F., 2003. Evolution of El Nino-precipitation relationships from satellites and gauges. J. Geophys. Res. 108 (D4), 4153. http://dx.doi.org/10.1029/2002JD002690.
DeMaria, M., DeMaria, R.T., Knaff, J.A., Molenar, D., 2012. Tropical cyclone lightning and rapid intensity change. Mon. Weather Rev. 140, 1828–1842.
Dowden, R.L., Brundell, J.B., Rodger, C.J., 2002. VLF lightning location by time of group arrival (TOGA) at multiple sites. J. Atmos. Sol. Terr. Phys. 64, 817–830.
Enno, S.E., 2011. A climatology of cloud-to-ground lightning over Estonia, 2005–2009. Atmos. Res. 100, 310–317.
Garreaud, R.D., Nicora, M.G., Bürgesser, R.E., Ávila, E.E., 2014. Lightning in Western Patagonia. J. Geophys. Res. Atmos. 119, 4471–4485.
Goodman, S.J., Buechler, D.E., Knupp, K., Driscoll, K., McCaul Jr., E.W., 2000. The 1997-98 El Nino event and related wintertime lightning variations in the southeastern United States. Geophys. Res. Lett. 27, 541–544.
Hamid, E.Y., Kawasaki, Z.-I., Mardiana, R., 2001. Impact of the 1997–98 El Nino event on lightning activity over Indonesia. Geophys. Res. Lett. 28, 147–150.
Hidayat, S., Ishii, M., 1998. Spatial and temporal distribution of lightning activity around Java. J. Geophys. Res. Atmos. 103, 14001–14009.
Holle, R.L., 2014. Diurnal variations of NLDN-reported cloud-to-ground lightning in the United States. Mon. Weather Rev. 142, 1037–1052.
Hutchins, M.L., Holzworth, R.H., Brundell, J.B., Rodger, C.J., 2012. Relative detection efficiency of the World Wide Lightning Location Network. Radio Sci. 47, RS6005. http://dx.doi.org/10.1029/2012RS005049.
Hutchins, M.L., Holzworth, R.H., Virts, K.S., Wallace, J.M., Heckman, S., 2013. Radiated VLF energy differences of land and oceanic lightning. Geophys. Res. Lett. 40, 2390–2394.
Iwasaki, H., 2014. Preliminary study on features of lightning discharge around Japan using World Wide Lightning Location Network data. SOLA 10, 98–102.
Iwasaki, H., 2016. Relating lightning features and topography over the Tibetan Plateau using the World Wide Lightning Location Network data. J. Meteorol. Soc. Jpn. 91, 431–442.
Jacobson, A.R., Holzworth, R.H., Harlin, J., Dowden, R.L., Lay, E.H., 2006. Performance assessment of the World Wide Lightning Location Network (WWLLN), using the Los Alamos Sferic Array (LASA) as ground truth. J. Atmos. Ocean. Technol. 23, 1082–1092.
Jiang, H., Ramirez, E.M., Cecil, D.J., 2013. Convective and rainfall properties of tropical cyclone inner cores and rainbands from 11 years of TRMM data. Mon. Weather Rev. 141, 431–450.
Johnson, R.H., Ciesielski, P.E., 2002. Characteristics of the 1998 summer monsoon onset over the northern South China Sea. J. Meteorol. Soc. Jpn. 80, 561–578.
Kandalgaonkar, S.S., Tinmaker, M.I.R., Kulkarni, J.R., Nath, A., Kulkarni, M.K., Trimbake, H.K., 2005. Spatio-temporal variability of lightning activity over the Indian region. J. Geophys. Res. 110, D11108. http://dx.doi.org/10.1029/2004JD005631.
Kucienska, B., Raga, G.B., Rodriguez, O., 2010. Cloud-to-ground lightning over Mexico and adjacent oceanic regions: a preliminary climatology using the WWLLN dataset. Ann. Geophys. 28, 2047–2057.
Kuleshov, Y., Mackerras, D., Darveniza, M., 2006. Spatial distribution and frequency of lightning activity and lightning flash density maps for Australia. J. Geophys. Res. 111, D19105. http://dx.doi.org/10.1029/2005JD006982.
Kumar, P.R., Kamra, A.K., 2012. Variability of lightning activity in South/Southeast Asia during 1997–98 and 2002–03 El Nino/La Nina events. Atmos. Res. 118, 84–102.
Lay, E.H., Holzworth, R.H., Rodger, C.J., Thomas, J.N., Pinto Jr., O., Dowden, R.L., 2004. WWLL global lightning detection system: regional validation study in Brazil. Geophys. Res. Lett. 31, L03102. http://dx.doi.org/10.1029/2003GL018882.
Lay, E.H., Jacobson, A.R., Holzworth, R.H., Rodger, C.J., Dowden, R.L., 2007. Local time variation in land/ocean lightning flash density as measured by the World Wide Lightning Location Network. J. Geophys. Res. Atmos. 112, D13111. http://dx.doi.org/10.1029/2006JD007944.
Ma, M., Tao, S., Zhu, B., Lv, W., 2005. The anomalous variation of the lightning activity in southern China during the 1997/98 El Niño event. Sci. China Ser. D Earth Sci. 48, 1537–1547.
Makela, A., Rossi, P., Schultz, D.M., 2011. The daily cloud-to-ground lightning flash density in the contiguous United States and Finland. Mon. Weather Rev. 139, 1323–1337.
Molinari, J., Moore, P., Idone, V., 1999. Convective structure of hurricanes as revealed by lightning locations. Mon. Weather Rev. 127, 520–534.
Mori, S., et al., 2004. Diurnal land–sea rainfall peak migration over Sumatera Island, Indonesian Maritime Continent, observed by TRMM satellite and intensive raw in sonde soundings. Mon. Weather Rev. 132, 2021–2039.
Nesbitt, S.W., Zipser, E.J., 2003. The diurnal cycle of rainfall and convective intensity according to three years of TRMM measurements. J. Clim. 16, 1456–1475.
Orville, R.E., Huffines, G.R., 2001. Cloud-to-ground lightning in the United States: NLDN results in the first decade, 1989–98. Mon. Weather Rev. 129, 1179–1193.
Pan, L., Qie, X., Liu, D., Wang, D., Yang, J., 2010. The lightning activities in super typhoons over the Northwest Pacific. Sci. China Ser. D Earth Sci. 53 (8), 1241–1248.
Pan, L., Liu, D., Qie, X., Wang, D., Zhu, R., 2013. Land-sea contrast in the lightning diurnal variation as observed by the WWLLN and LIS/OTD data. Acta Meteorol. Sin. 27 (4), 591–600.
Pan, L., Qie, X., Wang, D., 2014. Lightning activity and its relation to the intensity of typhoons over the Northwest Pacific Ocean. Adv. Atmos. Sci. 31 (3), 581–592.
Pessi, A.T., Businger, S., 2009. Relationships among lightning, precipitation, and hydrometeor characteristics over the North Pacific Ocean. J. Appl. Meteorol. Climatol. 48, 833–848.
Poelman, D.R., 2014. A 10-year study on the characteristics of thunderstorms in Belgium based on cloud-to-ground lightning data. Mon. Weather Rev. 142, 4839–4849.
Qian, J.-H., 2008. Why precipitation is mostly concentrated over islands in the Maritime Continent. J. Atmos. Sci. 65, 1428–1441.
Qie, X., Toumi, R., Yuan, T., 2003. Lightning activities on the Tibetan Plateau as observed by the lightning imaging sensor. J. Geophys. Res. 108, 4551. http://dx.doi.org/10.1029/2002JD003304.
Ren, H., Sun, C., Ren, F., Yu, Y., Lu, B., Tian, B., et al., 2017. Identification method for El Nino/La Nina events. GB/T 33666-2017, Beijing. pp. 4.
Rodger, C.J., Brundell, J.B., Dowden, R.L., Thomson, N.R., 2004. Location accuracy of long distance VLF lightning location network. Ann. Geophys. 22, 747–758.
Rodger, C.J., Brundell, J.B., Dowden, R.L., 2005. Location accuracy of VLF World-Wide Lightning Location (WWLL) network: post-algorithm upgrade. Ann. Geophys. 23 (2), 277–290.
Rudlosky, S.D., Shea, D.T., 2013. Evaluating WWLLN performance relative to TRMM/LIS. Geophys. Res. Lett. 40, 2344–2348.
Rutledge, S.A., Williams, E.R., Keenan, T.D., 1992. The Down Under Doppler and Electricity Experiment (DUNDEE) overview and preliminary results. Bull. Am. Meteorol. Soc. 73, 3–16.
Satori, G., Williams, E., Lemperger, I., 2009. Variability of global lightning activity on the ENSO time scale. Atmos. Res. 91, 500–507.
Song, J.-J., Wang, Y., Wu, L., 2010. Trend discrepancies among three best track data sets of western North Pacific tropical cyclones. J. Geophys. Res. Atmos. 115, D12128. http://dx.doi.org/10.1029/2009JD013058.
Soula, S., Kasereka, J.K., Georgis, J.F., Barthe, C., 2016. Lightning climatology in the Congo Basin. Atmos. Res. 178-179, 304–319.
Squires, K., Businger, S., 2008. The morphology of eyewall lightning outbreaks in two category 5 hurricanes. Mon. Weather Rev. 136, 1706–1726.
Stevenson, S.N., Corbosiero, K.L., DeMaria, M., Vigh, J.L., 2018. A 10-year survey of tropical cyclone inner-core lightning bursts and their relationship to intensity change. Weather Forecast. 33, 23–36.
Taszarek, M., Czernecki, B., Koziol, A., 2015. A cloud-to-ground lightning climatology for Poland. Mon. Weather Rev. 143, 4285–4304.
Thornton, J.A., Virts, K.S., Holzworth, R.H., Mitchell, T.P., 2017. Lightning enhancement over major oceanic shipping lanes. Geophys. Res. Lett. 44. http://dx.doi.org/10.1002/2017GL074982.
Tsurushima, D., Sakaida, K., Honma, N., 2017. Spatial distribution of cold-season lightning frequency in the coastal areas of the Sea of Japan. Prog. Earth Planet. Sci. 4. http://dx.doi.org/10.1186/s40645-017-0122-0.
Venugopal, V., Virts, K., Sukhatme, J., Wallace, J.M., Chattopadhyay, B., 2016. A comparison of the fine-scale structure of the diurnal cycle of tropical rain and lightning. Atmos. Res. 169, 511–515.
Virts, K.S., Thornton, J.A., Wallace, J.M., Hutchins, M.L., Holzworth, R.H., Jacobson, A.R., 2011. Daily and intraseasonal relationships between lightning and NO_2 over the Maritime Continent. Geophys. Res. Lett. 38, L19803. http://dx.doi.org/10.1029/2011GL048578.
Virts, K.S., Wallace, J.M., Hutchins, M.L., Holzworth, R.H., 2013a. Diurnal lightning variability over the Maritime Continent: impact of low-level winds, cloudiness, and the MJO. J. Atmos. Sci. 70, 3128–3146.
Virts, K.S., Wallace, J.M., Hutchins, M.L., Holzworth, R.H., 2013b. Highlights of a new ground-based, hourly global lightning climatology. Bull. Am. Meteorol. Soc. 94, 1381–1391.
Virts, K.S., Wallace, J.M., Hutchins, M.L., Holzworth, R.H., 2015. Diurnal and seasonal lightning variability over the Gulf stream and the Gulf of Mexico. J. Atmos. Sci. 72, 2657–2665.
Wang, B., Chan, J.C.L., 2002. How strong ENSO events affect tropical storm activity over the Western North Pacific. J. Clim. 15, 1643–1658.
Wang, F., Qie, X., Liu, D., Shi, H., Srivastava, A., 2016. Lightning activity and its relationship with typhoon intensity and vertical wind shear for Super Typhoon Haiyan (1330). J. Meteorol. Res. 30 (1), 117–127.
Williams, E.R., 2005. Lightning and climate: a review. Atmos. Res. 76, 272–287.
Williams, E.R., Rutledge, S.A., Geotis, S.G., Renno, N., Rasmussen, E., Rickenbach, T., 1992. A radar and electrical study of tropical “hot towers”. J. Atmos. Sci. 49, 1386–1395.
Willoughby, H.E., Clos, J.A., Shoreibah, M.G., 1982. Concentric eye walls, secondary wind maxima, and the evolution of the hurricane vortex. J. Atmos. Sci. 39, 395–411.
Xu, W., Zipser, E.J., Liu, C., 2009. Rainfall characteristics and convective properties of mei-yu precipitation systems over South China, Taiwan, and the South China Sea. Part I: TRMM observations. Mon. Weather Rev. 137, 4261–4275.
Xu, W., Rutledge, S.A., Zhang, W., 2017. Relationships between total lightning, deep convection, and tropical cyclone intensity change. J. Geophys. Res. Atmos. 122, 7047–7063.
Yang, G.-Y., Slingo, J., 2001. The diurnal cycle in the Tropics. Mon. Weather Rev. 129, 784–801.
Yang, X., Sun, J., Li, W., 2015. An analysis of cloud-to-ground lightning in China during 2010–13. Weather Forecast. 30, 1537–1550.

Yoshida, S., Morimoto, T., Ushio, T., Kawasaki, Z., 2007. ENSO and convective activities in Southeast Asia and western Pacific. Geophys. Res. Lett. 34, L21806. http://dx.doi.org/10.1029/2007GL030758.

Yuan, T., Qie, X., 2008. Study on lightning activity and precipitation characteristics before and after the onset of the South China Sea summer monsoon. J. Geophys. Res. 113, D14101. http://dx.doi.org/10.1029/2007JD009382.

Zhang, W., Zhang, Y., Zheng, D., Zhou, X., 2012. Lightning distribution and eyewall outbreaks in tropical cyclones during landfall. Mon. Weather Rev. 140, 3573–3586.

Zhang, W., Zhang, Y., Zhou, X., 2013. Lightning activity and precipitation characteristics of Typhoon Molave (2009) around its landfall. Acta Meteorol. Sin. 27 (5), 742–757.

Zhang, W., Zhang, Y., Zheng, D., Wang, F., Xu, L., 2015. Relationship between lightning activity and tropical cyclone intensity over the northwest Pacific. J. Geophys. Res. Atmos. 120, 4072–4089.

Zheng, D., Zhang, Y., Meng, Q., Chen, L., Dan, J., 2016. Climatological comparison of small- and large-current cloud-to-ground lightning flashes over Southern China. J. Clim. 29, 2831–2848.

Zipser, E.J., 1994. Deep cumulonimbus cloud systems in the Tropics with and without lightning. Mon. Weather Rev. 122, 1837–1851.

Zipser, E.J., Liu, C., Cecil, D.J., Nesbitt, S.W., Yorty, D.P., 2006. Where are the most intense thunderstorms on earth? Bull. Am. Meteorol. Soc. 87, 1057–1071.